A Novel Fluorophore with Dual Fluorescence: Local Excited State and Photoinduced Electron-Transfer-Promoted Charge-Transfer State

ARTICLE *in* CHEMPHYSCHEM · AUGUST 2004

Impact Factor: 3.42 · DOI: 10.1002/cphc.200400064 · Source: PubMed

4 AUTHORS:

Viruthachalam Thiagarajan
Bharathidasan University
26 PUBLICATIONS **468** CITATIONS
SEE PROFILE

Selvaraju Chellappan
University of Madras
5 PUBLICATIONS **88** CITATIONS
SEE PROFILE

E. J. Padma Malar
University of Madras
62 PUBLICATIONS **538** CITATIONS
SEE PROFILE

Perumal Ramamurthy
University of Madras
110 PUBLICATIONS **1,844** CITATIONS
SEE PROFILE

CHEMPHYSCHEM

A Novel Fluorophore with Dual Fluorescence: Local Excited State and Photoinduced Electron-Transfer-Promoted Charge-Transfer State

Viruthachalam Thiagarajan,[a] Chellappan Selvaraju,[b] E. J. Padma Malar,[c] and Perumal Ramamurthy*[a, b]

Absorption and emission spectra of 9-N,N-dimethylaniline decahydroacridinedione (DMAADD) have been studied in different solvents. The fluorescence spectra of DMAADD are found to exhibit dual emission in aprotic solvents and single emission in protic solvents. The effect of solvent polarity and viscosity on the absorption and emission spectra has also been studied. The fluorescence excitation spectra of DMAADD monitored at both the emission bands are different. The presence of two different conformation of the same molecule in the ground state has lead to two close lying excited states, local excited (LE) and charge transfer (CT), and thereby results in the dual fluorescence of the dye. A CT state involving the N,N-*dimethylaniline group and the decahydroacridinedione chromophore as donor and acceptor, respectively, has been identified as the source of the long wavelength anomalous fluorescence. The experimental studies were supported by ab initio time dependent-density functional theory (TD-DFT) calculations performed at the B3LYP/6–31G* level. The molecule possesses photoinduced electron transfer (PET) quenching in the LE state, which is confirmed by the fluorescence lifetime and fluorescent intensity enhancement in the presence of transition metal ions.*

Introduction

The understanding of the dual fluorescence of certain aromatic molecules has greatly advanced in recent years. Since Lippert's initial discovery[1] of the dual fluorescent behaviour of 4-(*N*,*N*-dimethylamino)benzonitrile (DMABN), various theories have been proposed to explain the anomalous, long wavelength fluorescence, including solute–solvent exciplex formation,[2] twisted intramolecular charge transfer (TICT),[3] rehybridisation of the acceptor (RICT)[4] and planar intramolecular charge transfer (PICT).[5] Among the mechanisms discussed, the most prominent one is the TICT model put forward by Grabowski et al. In essence, it states that intramolecular charge transfer occurs from the dimethylamino donor group to the phenyl acceptor ring and that this process is accompanied by a twisting motion and orbital decoupling of the phenyl acceptor ring.[6] TICT state formation depends upon polarity and viscosity of the medium and the electron-donor–acceptor properties of the molecules.[7]

Recently, Zachariase et al proposed a PICT model which assumes the intramolecular charge transfer state to be in a planar conformation, whereas the local excited state retains at least a part of the pyramidal structure of the dimethylamino group present in the electronic ground state.[8] In the PICT model, the energy gap between the two lowest singlet excited states $\Delta E(S_1$ and $S_2)$ is sufficiently small. A dynamic state reversal can occur on excitation of the molecule in a polar medium, which leads to an emitting CT state along with the LE state and, hence, a dual fluorescence.[5]

Electron transfer (ET) is the most elementary and unique of all chemical reactions, and it also plays a crucial role in many essential biological processes.[9] One significant type of ET is the photoinduced ET (PET), which can translate the effect of binding an analyte to a visible change of the fluorescence output. In the absence of the analyte, the fluorescence is quenched due to PET between the receptor and the fluorophore; whereas upon binding of the cation, the thermodynamics of the quenching process is rendered unfavourable, and the fluorescence emission is switched on.[10] Therefore, to design a fluorescent probe, a cation-specific receptor acting as the electron donor must be combined with a fluorophore that matches the appropriate reduction potential.

Decahydroacridinedione (ADD) dyes have been reported as a new class of laser dyes with lasing efficiency comparable to that of coumarin-102, and these dyes have structural similarities with NADH.[11] These dyes have been shown to mimic the NADH analogs to greater extent because of their tricyclic structure, which is capable of protecting the enamine moiety.[12]

[a] *V. Thiagarajan, Dr. P. Ramamurthy*
Department of Inorganic Chemistry
University of Madras, Guindy Campus
Chennai-600 025 (India)
Fax: (+91) 249-250-06
E-mail: prm60@hotmail.com

[b] *Dr. C. Selvaraju, Dr. P. Ramamurthy*
National Centre for Ultrafast Processes
University of Madras, Taramani Campus
Chennai-600 113 (India)

[c] *Dr. E. J. P. Malar*
Research Scientist, University Grants Commission
Department of Physical Chemistry
University of Madras, Guindy Campus
Chennai-600 025 (India)

  DOI: 10.1002/cphc.200400064

The photophysical and photochemical properties of ADD dyes in solution and in PMMA matrix have been extensively studied.[13]

We present here the first nonconjugated but covalently linked bichromophoric system (DMAADD) that shows dual fluorescence along with large fluorescence enhancement in the presence of transition metal ions. In DMAADD, the *N*,*N*-dimethylaniline group and the ADD fluorophore act as electron donor and acceptor, respectively (Scheme 1).

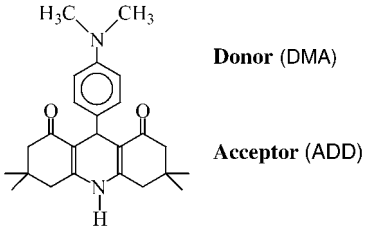

Scheme 1. *DMAADD.*

The photophysical properties of a new dual-emitting decahydroacridinedione derivative, DMAADD, have been studied by steady-state absorption and fluorescence spectroscopy. The electron-transfer thermodynamics have been estimated on the basis of the spectroscopic data and redox potentials.

Results and Discussion

Absorption and emission spectral studies of DMAADD in a series of protic and aprotic solvents have been carried out. Table 1 presents the absorption and fluorescence characteristics of DMAADD dye. The absorption spectra of DMAADD in methanol and acetonitrile are depicted in Figure 1. The absorption spectra of DMAADD are very similar in all aprotic solvents, which show a strong absorption around 360 nm, and this band has been assigned to the charge transfer from the ring nitrogen to the ring carbonyl oxygen centre in the ADD fluorophore (LE).[13] A shoulder in the shorter wavelength region is observed around 300 nm, and this is assigned to the intramolecular transition of the *N*,*N*-dimethylaniline group. However, in protic solvents like methanol, the shoulder disappears due to the protonation of the *N*,*N*-dimethylaniline (DMA) group, which in turn leads to the blue shift of the DMA absorption.

Table 1. *Absorption and fluorescence spectral maxima and Stokes shift of DMAADD in various solvents.*

Solvent	Absorption λ_{max} [nm]	Fluorescence [nm] λ_{max} (LE)	λ_{max} (CT)	Stokes shift [cm^{-1}] $\Delta\nu$ (LE)	$\Delta\nu$ (CT)
benzene	354	400	516	3249	8869
dichloromethane	360	420	537	3968	9156
acetone	360	424	548	4193	9530
acetonitrile	362	424	566	4039	9956
DMF	366	427	562	3903	9529
methanol	374	445		4266	

The emission spectra were recorded in different solvents by exciting the dye at its longer wavelength absorption maximum. The emission spectra recorded in various solvents are shown in Figure 2. The emission spectrum of DMAADD shows a single peak in protic solvents and two distinct peaks in aprotic solvents—a shorter wavelength LE fluorescence (B state) around 424 nm due to ADD fluorophore[13] and a new anomalous longer wavelength fluorescence (A state) around 550 nm. In comparison with the LE state, the new longer wavelength broad band emission is found to shift towards lower energies with increasing solvent polarity; this shift is due to the stabilisation of the CT state. Interestingly, on removal of methyl groups from DMAADD (in the donor), the A-state emission shows a blue shift accompanied by a decrease in the emission intensity.[14] This happens because the energy position of a pure charge-transfer transition is a linear function of the ionisation potential of the donor moiety.[15] These observations are consistent with charge-transfer characteristics of the A state.

Solvatochromic Shift and Excited-State Dipole Moments

The red shift observed in the fluorescence spectra with an increase in solvent polarity depends on the difference in permanent dipole moments of the ground and excited state, and this is in accordance with the theory of dielectric polarisation.[16] The effect of solvent polarity on the fluorescence shift was utilised to infer the charge separation of DMAADD in the excited state. If the dipole moments are approximated by point dipoles in the centre of the spherical cavity with radius *a* and the mean solute polarisability is neglected, one obtains [Equation (1)][17]

$$\bar{\nu}_f = \bar{\nu}_f^{vac} - \frac{2\mu_e(\mu_e - \mu_g)}{hca^3}F \qquad (1)$$

where ν_f and ν_f^{vac} are the spectral positions of the solvent equilibrated fluorescence maxima and the value extrapolated to gas phase conditions, respectively; μ_e and μ_g are dipole moments in the excited and ground states, respectively. *h* and *c* are Plank's constant and the speed of light, respectively. The Lippert-Mataga solvent polarity parameter, (*F*) is given by the following expression [Equation (2)],

$$F = \frac{D-1}{2D+1} - {}^1\!/_2\left(\frac{n^2-1}{2n^2+1}\right) \qquad (2)$$

where *D* and *n* are the dielectric constant and the refractive index of the solvent, respectively.

The Onsagar cavity radius, *a*, was estimated using PCMODEL software. This software assumes the molecule to be spherical and calculated the total surface area (TSA) of the molecule.

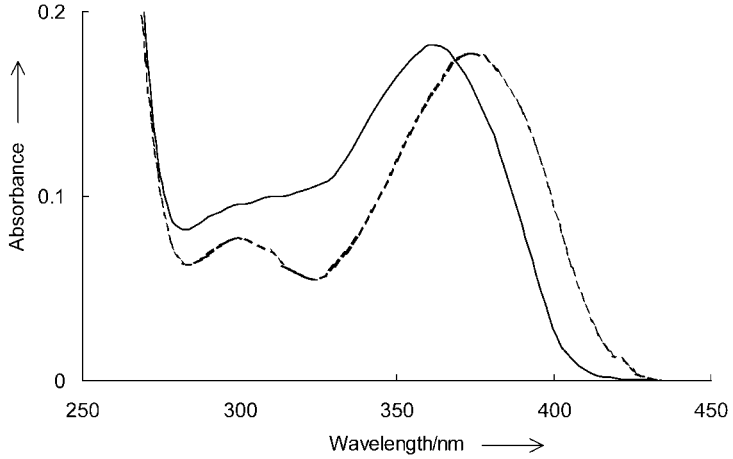

Figure 1. *Absorption spectrum of DMAADD in acetonitrile (——) and methanol(-----).*

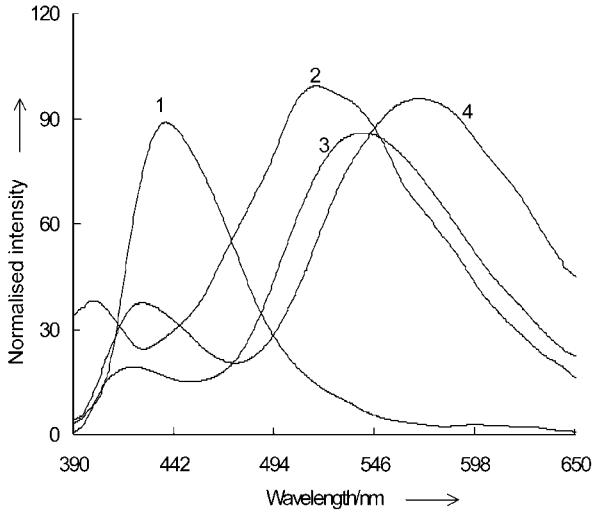

Figure 2. *Emission spectrum of DMAADD in different solvents 1) methanol, 2) benzene, 3) dichloromethane, 4) acetonitrile.*

From the calculated total surface area the radius can be obtained using Equation (3).

$$a = \left(\frac{\mathrm{TSA}}{4\pi}\right)^{1/2} \tag{3}$$

The plot of fluorescence shift of A and B states versus F gives a straight line. The slope of the straight line, S, is represented by Equation (4).

$$S = \frac{2\mu_e(\mu_e - \mu_g)}{hca^3} \tag{4}$$

The plot of fluorescence shift versus Lippert–Mataga solvent polarity parameter for the B state and A state is shown in Figure 3. The slope (S) value is obtained by excluding the protic solvents, which may have some specific solute-solvent interactions. The value of a was found to be 5.302 Å. The slope obtained for the A and B states was found to be 9.978 and 0.845, respectively. The slope is about 12 times larger for the A state than that of the B-state emission, which is consistent with a larger CT character of the A state. The higher value of the slope is indicative of the fact that the intramolecular charge transfer leading to electron distribution in the excited state is more polar compared to the ground state for the A state ($\mu_e > \mu_g$). In general, the charge transfer within the decahydroacridinedione moiety, that is, from the central ring nitrogen atom to the carbonyl group (LE state), shows very little solvent induced red shift independent of the substituent in the nineth position.[13d]

Fluorescence Enhancement in the Presence of Transition Metal Ions

DMAADD is found to be very weakly fluorescent compared to the constituent fluorophores without the electron donor DMA group. This observation reveals that there is an intramolecular fluorescence quenching via PET from the electron rich amino moiety to the relatively electron deficient excited state of the ADD fluorophore. The thermodynamic feasibility of PET within DMAADD can be verified by means of the Rehm–Weller equation [Equation (5)].[18]

$$\Delta G_{\mathrm{PET}} = 23.06\,[E_{\mathrm{ox}}(\mathrm{receptor}) - E_{\mathrm{red}}(\mathrm{fluorophore})] - e^2/\varepsilon r - E_{00} \tag{5}$$

ΔG_{PET} is estimated as $-23.45\ \mathrm{kcal\,mol^{-1}}$ ($E_{ox} = 0.47$ V and $E_{red} = -1.49$ V and $E_{00} = 68.65\ \mathrm{kcal\,mol^{-1}}$), which suggests that the photoinduced intramolecular electron transfer reactions might occur. The ϕ_f values of DMAADD and ADD dye without the donor group in acetonitrile are found to be $\approx 0.0056(\pm$

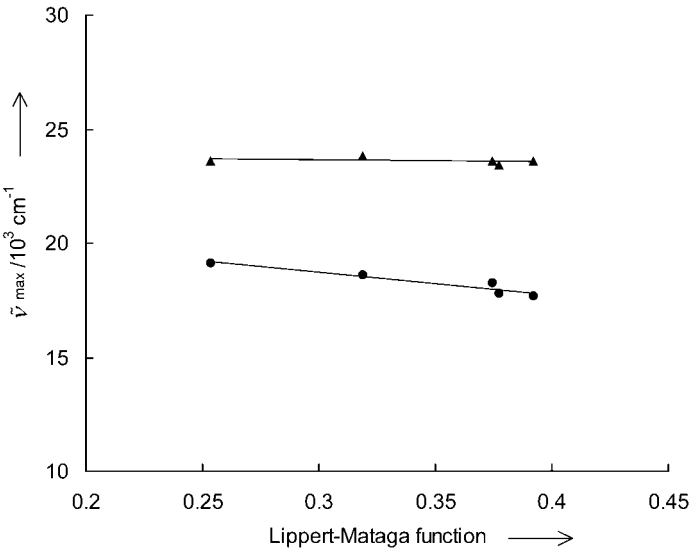

Figure 3. *Plot of fluorescence shift versus Lippert–Mataga solvent polarity parameter for DMAADD dye (● = A state, ▲ = B state).*

5%) and 0.91(±0.02) respectively. PET is quite efficient in DMAADD, and this is evident from its low fluorescence quantum yield in comparison with that of ADD dye without the donor moiety.

Figures 4 and 5 show the effect of Co(II) on the absorption and fluorescence spectra of DMAADD in acetonitrile. On the other hand, the maximum fluorescence enhancement (FE) for various metal ions are presented in Table 2. The disappearance of the DMA absorption around 300 nm in DMAADD in the presence of transition metal ions suggests that there is an interaction between the metal ion and the *N*,*N*-dimethylamino group in the ground state. Interestingly, the binding of transition metal ions with the lone pair of nitrogen atom has lead to FE in the B state without a spectral shift in the emission maximum accompanied with the disappearance of A-state fluorescence (cobalt(II) shows 323-fold fluorescence enhancement!). The PET process ceases when the amine receptor binds with the metal ion, resulting in the recovery of LE state fluorescence, which is shown clearly in Figure 5. Full recovery of the fluorescence takes place by the suppression of PET at the limiting concentration of the metal ions. Because some of the salts we used were in their hydrated forms, we purposely carried out blank experiments by taking small amounts of water in an acetonitrile solution of DMAADD. Addition of water leads to less than a one-fold increase in the fluorescence intensity of the LE state and rules out the possibility of fluorescence enhancement due to hydrated water molecules present in the salts.

Table 2. *Fluorescence output of DMAADD in acetonitrile with different transition-metal ion input.*[a]

Input Metal ion	Concentration[b] [M]	Output FE
Mn^{II}	1.3×10^{-3}	36
Fe^{II}	1.4×10^{-4}	198
Co^{II}	1.2×10^{-3}	323
Ni^{II}	1.0×10^{-3}	255
Cu^{II}	1.7×10^{-5}	108
Zn^{II}	7.0×10^{-5}	167

[a] Experimental conditions: concentration of the dye 1.6×10^{-5} mol dm^{-3}, $\lambda_{exc}=380$ nm at isosbestic point. [b] The concentration of the metal ion for which fluorescence enhancement is maximum.

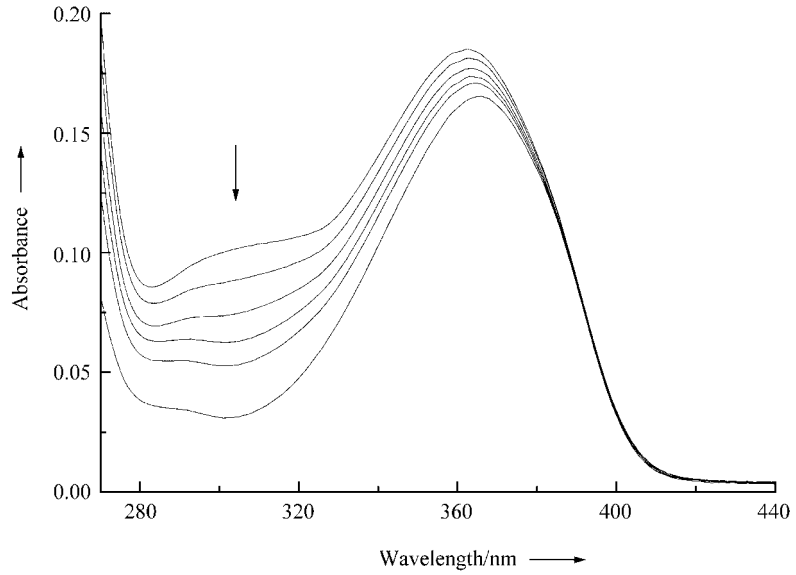

Figure 4. *Absorption spectra of DMAADD in acetonitrile in the presence and absence of $Co(ClO_4)_2$; the concentration of the metal ions is (from top to bottom) 0, 190, 390, 780, 1020 and 1200 μM.*

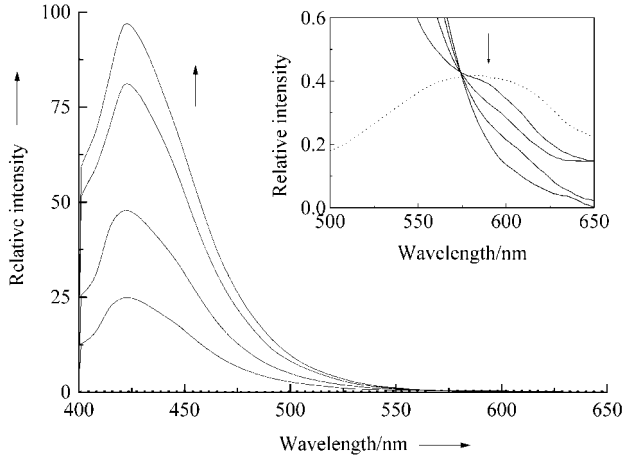

Figure 5. *Fluorescence enhancement of DMAADD in acetonitrile by $Co(ClO_4)_2$, $\lambda_{exc}=380$ nm. The concentration of the metal ions is (from bottom to top) 0, 190, 390, 780, and 1200 μM. Dye alone (·····). The inset shows the emission spectra in the region 500–650 nm.*

Fluorescence Lifetime

The emission decays, $I(t,\lambda)$, were fitted globally to a biexponential [Equation (6)],

$$I(t,\lambda) = \alpha_1(\lambda)\exp(-t/\tau_1) + \alpha_2(\lambda)\exp(-t/\tau_2) \quad (6)$$

where the two lifetimes (τ_1 and τ_2) were linked, and the pre-exponential factors (α_1 and α_2) varied freely. The two emissions have very different fluorescence lifetimes in acetonitrile, 0.66 ns and 1.98 ns for A and B states, respectively. Global analysis of the fluorescence decay at 14 different emission wavelengths in the region 400–530 nm at 10 nm intervals yielded lifetimes for both the components. The fractional contributions from these decay times at the different emission wavelengths are compiled in Table 3. Above 530 nm, only the A-state lifetime is observed (0.66 ns). The biexponential nature of the fluorescence decay at wavelengths below 530 nm is due to the overlapping of the A-state fluorescence with the fluorescence band of the B state. The pre-exponential factor of the longer-lifetime component decreases while the pre-exponential factor of the short-lived component increases on monitoring the decay from 430 nm to 530 nm, after which only the short-lived component exists. This confirms the overlap of the two states.

Table 3. Lifetimes and pre-exponential factors (in parentheses) obtained by global analysis of the fluorescence decays of DMAADD in acetonitrile[a], at different observation wavelengths.

λ_{em} [nm]	τ_1 [ns]	τ_2 [ns]
400	0.66(0.41)	1.98(0.59)
410	0.66(0.37)	1.98(0.63)
420	0.66(0.36)	1.98(0.64)
430	0.66(0.24)	1.98(0.76)
440	0.66(0.27)	1.98(0.73)
450	0.66(0.28)	1.98(0.72)
460	0.66(0.32)	1.98(0.62)
470	0.66(0.58)	1.98(0.42)
480	0.66(0.75)	1.98(0.25)
490	0.66(0.87)	1.98(0.13)
500	0.66(0.94)	1.98(0.06)
510	0.66(0.96)	1.98(0.04)
520	0.66(0.98)	1.98(0.02)
530	0.66(0.99)	1.98(0.01)

[a] $\lambda_{exc}=375$ nm, $\chi_g^2=1.5171$. Decay curves with 1×10^4 counts at the maximum.

We studied the effect of transition-metal ions on the fluorescence decay of DMAADD system in acetonitrile. The shorter-lived component disappears gradually in the presence of the metal ions, and the longer-lived component lifetime increases (1.98 ns to 2.70 ns) along with an increase in the amplitude. An increase in the lifetime of the longer-lived component in the presence of metal ions and the disappearance of the shorter-lived component is in accordance with the metal-ion-induced suppression of PET in the DMAADD system. At the limiting concentration (Table 2) of metal ion, we observed the full recovery of the long-lived component (2.70 ns) with complete disappearance of the short-lived component.

Fluorescence Quenching of A State by Methanol

In Figure 6 the fluorescence decay of DMAADD in pure acetonitrile and in acetonitrile/methanol mixtures monitored at 650 nm is shown. The fluorescence quenching of DMAADD in acetonitrile by methanol was analysed using the Stern–Volmer equation [Eq. (7)],

$$\tau_0/\tau = 1 + k_q\tau[Q] \qquad (7)$$

where τ_0 and τ are the fluorescence lifetime of DMAADD in the absence and presence of methanol, respectively, and Q is the concentration of methanol. The inset of Figure 6 shows the Stern–Volmer plot of DMAADD in acetonitrile quenched by methanol. From the fluorescence lifetime, the bimolecular quenching constant was found to be $3.6\times10^{12}\,\text{M}^{-1}\text{s}^{-1}$ for methanol. This value is larger than a diffusion-controlled reaction, and therefore, the hydrogen-bonding interaction between the methanol and the donor moiety should be taken into account. The above result is also supported by the disappearance of A-state fluorescence in methanol.

Nature of the CT State

The intensity ratio (I_A/I_B) of the emission bands at the respective emission maximum in acetonitrile does not change upon increasing the concentration of the DMAADD over the range

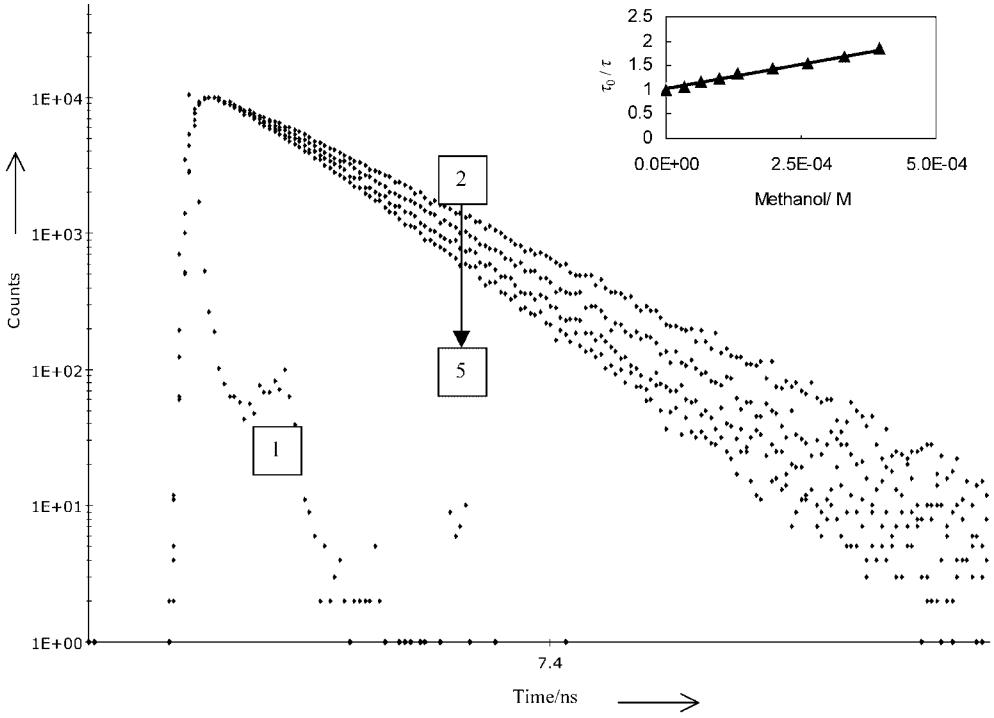

Figure 6. Fluorescence decay profiles of DMAADD at different concentration of methanol in acetonitrile, $\lambda_{ex}=375$ nm and $\lambda_{em}=650$ nm. 1) laser profile, 2) DMAADD alone (top), 3) 65.8, 4) 132, 5) 197 μM methanol (bottom). Inset shows the plot of τ_0/τ vs [Methanol].

of 10^{-6}–10^{-4} M. This rules out the possibilities of excimer and exciplex formation.

Is A-State Fluorescence due to a TICT?

In general TICT involves the rotation of the $-N(CH_3)_2$ group around the aromatic ring in the excited state. This type of rotation will be hindered in viscous solvents, and because of this, the fluorescence intensity of the TICT state should decrease with increasing viscosity of the solvent. To study the effect of viscosity on the DMAADD dye, the absorption and fluorescence spectra in dichloromethane containing varying percentage of polymethylmethacrylate (PMMA) were recorded. The absorption spectrum shows no significant change on PMMA addition. On the other hand, the emission spectra given in Figure 7 clearly shows the increase in the fluorescence intensity of the B state as the percentage of PMMA increases, whereas the A state fluorescence was found to remain constant throughout. Hence, the A-state emission in DMAADD cannot originate from the TICT state. The increase in B-state fluorescence intensity on increasing the viscosity of the medium is attributed to the decrease in the non-radiative deactivation of the B-state.

Is A-State Fluorescence due to an Excited-State Reaction or to Two Different Ground-State Species?

The observation of two different emission bands for a sample is either due to two different ground state species or one single species that undergoes a excited state reaction (for example, proton transfer, tautomerisation, etc.).

In place of a hydrogen atom on the amino group of the central ring nitrogen atom, we have an *n*-butyl group, and we found that there is no change in the A-state emission in aprotic solvents. This clearly rules out the anomalous longer wavelength emission which may result from the keto–enol tautomer.[14] Figure 8 shows the fluorescence excitation spectrum of DMAADD recorded at both of the emission maxima in acetonitrile. The fluorescence excitation spectra of DMAADD monitored at the corresponding emission maxima (A and B state) in acetonitrile, shows two distinctly different excitation bands: one at 370 nm, and the other at 360 nm, which correspond to the B and the A state, respectively. The excitation spectrum recorded at the longer wavelength emission maximum (A state) also shows a shoulder at 310 nm. The shoulder does not appear on the excitation spectrum recorded at the LE-state emission maximum (B state). The above result indicates that two different species are present in the ground state. To confirm this result, 3D emission spectral studies were performed. The 3D spectra recorded for DMAADD in methanol and acetonitrile are shown in Figure 9. In methanol, only one contour is observed for DMAADD. The corresponding excitation spectrum shows only one band at 370 nm, and the emission spectrum shows an emission at 430 nm. In acetonitrile, two contours were observed as shown in Figure 9b, and the corresponding excitation spectrum shows two bands at 370 and 360 nm. The excitation band observed at 370 nm corresponds to LE emission. The excitation band observed at 360 nm corresponds to CT emission (charge transfer between DMA and ADD fluorophore). The excitation and 3D spectra confirm the presence of two species of the same molecule in

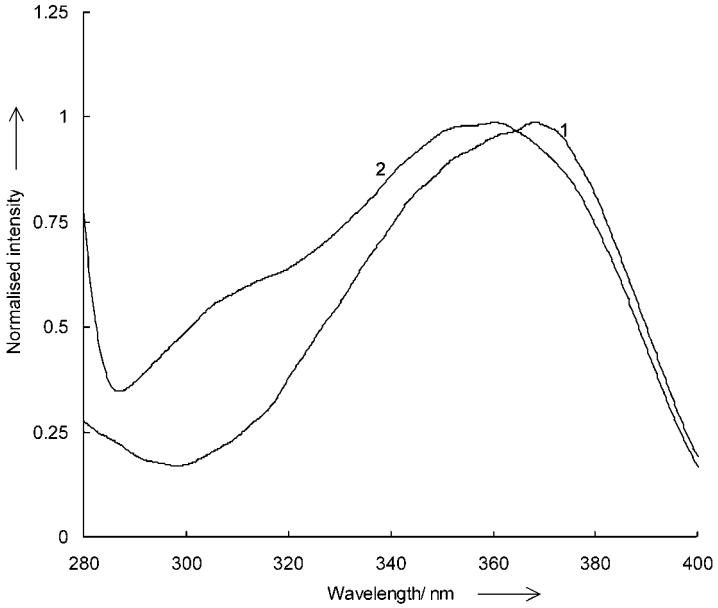

Figure 8. *Fluorescence excitation spectra of DMAADD in acetonitrile. 1) $\lambda_{em} = 424$ nm. 2) $\lambda_{em} = 566$ nm.*

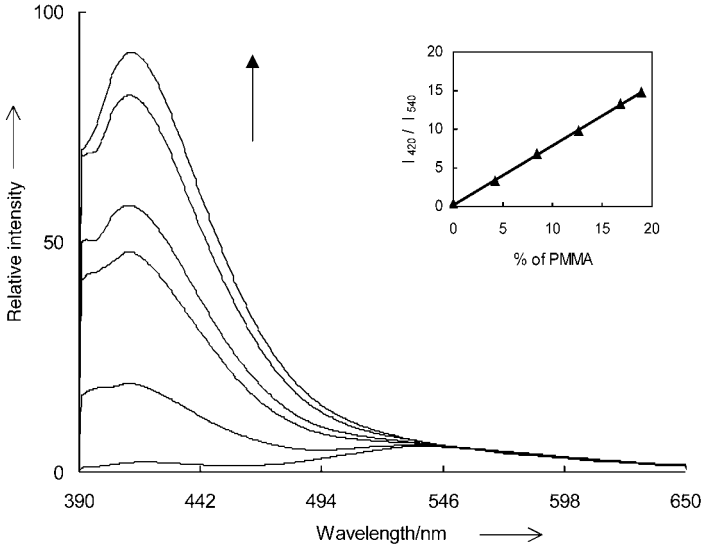

Figure 7. *Fluorescence spectra of DMAADD in dichloromethane containing various percentage of PMMA, $\lambda_{ex} = 362$ nm. The percentage PMMA is (bottom to top) 0, 4.2, 8.4, 12.6, 16.8, and 18.9.*

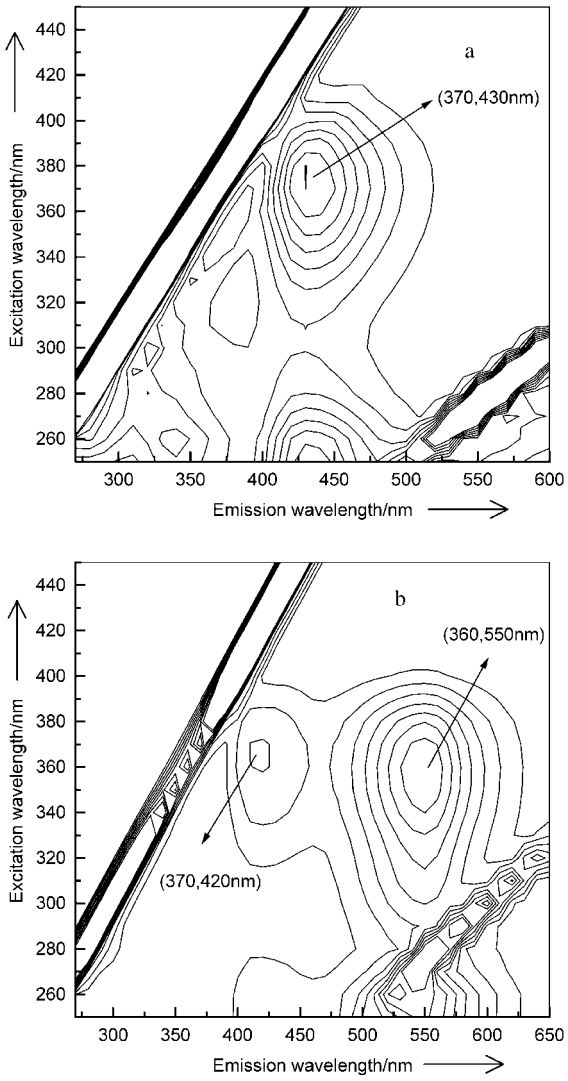

Figure 9. *3D spectra contour plot of DMAADD in a) methanol and b) acetonitrile.*

the ground state. The overlapping of electronic absorption of two species leads to the dual fluorescence at all wavelengths of excitation in the region 300–400 nm. At the blue edge of excitation, A-state fluorescence dominates, but at the red edge of excitation, B-state emission dominates.

The fluorescence decay analysis shows that the two-state decay is independent in nature and that there is no mother–daughter relationship between the two states. From the fluorescence lifetime results, it could be noted that all pre-exponential factors are positive, regardless of the emission wavelength. When the decay time of the A state is smaller than that of the B state and when the A state is formed out of the B state, the pre-exponential factor of the A state should be negative (rise time) at all wavelengths. Therefore, the absence of such a term in the time-resolved decay also supports the hypothesis that dual emission is not due to the excited-state reaction.

Quantum Chemical Analysis

To establish the nature of the two species, the electronic and geometrical structures of DMAADD were examined by hybrid Hartree–Fock (HF)/density functional theory (DFT) calculations using Gaussian 03 software.[19] The calculations invoked Becke's gradient corrected three-parameter exchange functional with the correlational functional of Lee, Yang, and Parr (B3 LYP)[20] and the split-valence polarised 6–31G* basis set.[21] Preliminary investigations at the semiempirical PM3 level[22] yielded two ground-state structures $S_0(\|)$ and $S_0(\perp)$ for DMAADD as shown in Figure 10.

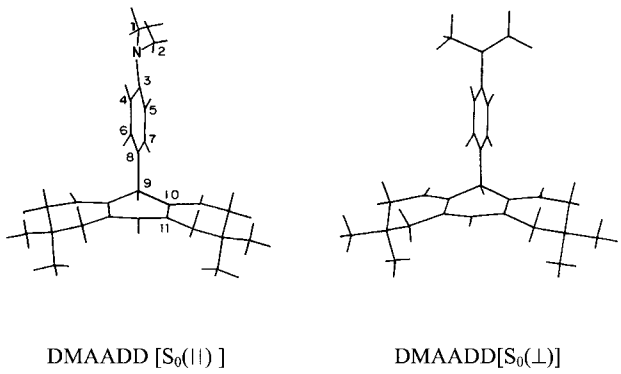

Figure 10. *DMAADD $S_0(\|)$ (left), and $S_0(\perp)$ (right)*

In both structures, the aniline part is found to be perpendicular to the acridine part, as observed crystallographically.[23] However, the two methyl carbon atoms of the *N*,*N*-dimethyl group lie in a plane parallel to that of the phenyl ring in $S_0(\|)$, whereas they lie in a perdendicular plane in $S_0(\perp)$. Vibrational frequency analysis by the PM3 method shows real values for all normal modes in $S_0(\|)$ and $S_0(\perp)$, which confirms that they are true minima in the potential energy surface.

Complete structural optimisation at the B3LYP/6–31G* level was carried out on the two ground-state structures of DMAADD, starting from the PM3 optimised $S_0(\|)$ and $S_0(\perp)$. The present ab initio results predict that the structure $S_0(\|)$ is 3.41 kcal mol^{-1} lower in energy than $S_0(\perp)$, which indicates that $S_0(\|)$ corresponds to the global minimum of DMAADD. In Table 4, we have presented selected dihedral angles of $S_0(\|)$ and $S_0(\perp)$ and compared them with the corresponding crystallographic values.[23] The B3LYP/6–31G* dihedral angles of $S_0(\|)$ agree closely with those observed experimentally.

Vertical excited singlet states $S_1(\|)$ and $S_1(\perp)$ were generated from B3LYP/6–31G* optimised ground states $S_0(\|)$ and $S_0(\perp)$ by the time-dependent DFT (TD-DFT) method.[24] The TD-DFT includes both single and double excitations for evaluating the energies of the excited states.[24a] Recent TD-DFT studies by Stratmann et al.[24a] and Fahrni et al.[25] have shown that this method yields reliable results. Herein, the lowest singlet-excited state is examined by taking into account all single and double excitations originating from the ten highest occupied molecular orbitals (MOs) to the ten lowest vacant MOs. The

Table 4. *Selected dihedral angles,[a] relative energies in $S_0(\|)$ and $S_0(\perp)$ and vertical excitation energies.*

State	Method	$C_4C_3NC_1$	$C_5C_3NC_2$	$C_{11}C_{10}C_9C_8$	Relative energy [kcal mol^{-1}]	Vertical excitation energy[b] [eV]
$S_0(\|)$	B3LYP/6–31G*	13.0(6.1 ± 9)	−13.2(−6.1 ± 9)	−106.4(−114.9 ± 6)	0.0	–
$S_0(\perp)$	B3LYP/6–31G*	−115.1	−64.8	−107.4	3.41	–
$S_1(\|)$	TD-B3LYP/6–31G*	13.0	−13.2	−106.4	–	2.89(2.40)
$S_1(\perp)$	TD-B3LYP/6–31G*	115.1	−64.8	−107.4	–	3.50(3.10)

[a] Dihedral angles reported from crystal structure are shown inside parentheses. For clarity, numbering of the carbon atoms is started from the donor group (not according to the nomenclature). [b] Experimentally observed emission energies in the solvent benzene are shown inside parentheses.

TD-DFT study shows that the vertical $S_1(\|)$ is a CT state originating from the highest occupied molecular orbital (HOMO) to the lowest unoccupied molecular orbital (LUMO) excitation. The HOMO is localised on the *N*,*N*-dimethyl aniline fragment (donor), and the LUMO is localised on the acridine part (acceptor). On the other hand, the nature of excitation involved in the state $S_1(\perp)$ is significantly different. This state is formed by mixing different single excited configurations, and the predominant one involves (HOMO-2)→LUMO excitation. The occupied HOMO-2 level is delocalised between the donor and acceptor moieties, while the LUMO is essentially localised on the acceptor fragment. Figure 11 shows a plot of the MOs generated by MOPLOT software.

The present calculations predict that the A state (CT), $S_1(\|)$, has an excitation energy of 2.89 eV, which is comparable to the experimental energy of 2.4 eV in benzene. The TD-DFT excitation energy of $S_1(\perp)$ is found to be about 0.6 eV higher than that in $S_1(\|)$. It may be interesting to note that the energy difference predicted between the $S_1(\|)$ and $S_1(\perp)$ states agrees closely with that observed experimentally (Table 4).

The PET from the donor moiety to the excited state of the decahydroacridinedione (acceptor) has lead to an emissive CT state that is responsible for the longer wavelength A-state fluorescence. The CT state has larger dipole moments than those of the S_0 and LE states; therefore, the relative energy of the CT state to that of the LE state depends upon the solvent polarity. In aprotic solvents such as acetonitrile, the CT state is lower in energy than that of the LE state, and this leads to dual fluorescence. In protic solvents such as methanol, the hydrogen-bonding interaction of the donor amino group with the solvent molecules results in the increase of the ionisation potential of the donor group, and hence, the CT state (A-state) energy is raised above the LE state. There is no overlap between the LE and CT states in methanol, and this leads to the emission from the LE state alone.

A comparison of the present experimental and theoretical studies on DMAADD indicates that the dual emission observed may originate from the two different conformations of the same molecule.

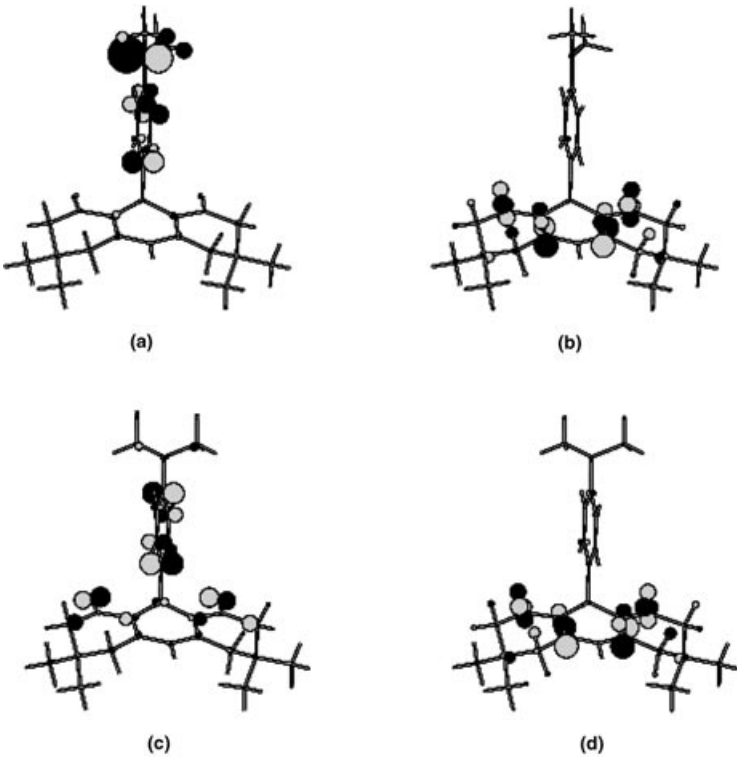

Figure 11. *Molecular orbital plots for the parallel and perpendicular conformations of the DMAADD system. a) HOMO (‖), b) LUMO (‖), c) HOMO-2 (⊥), d) LUMO (⊥).*

Conclusions

The bichromophoric system DMAADD exhibits dual fluorescence in aprotic solvents. The effect of solvent polarity and viscosity reveals that the charge-transfer nature of the A-state fluorescence is not due to TICT. The observation based on the excitation and 3D spectral studies clearly suggests that the dual emission is due to the existence of the two different conformers of DMAADD. The experimental emission energy of the above conformers agreed well with the values calculated by the TD-DFT method at the B3LYP/6–31G* level. The dual fluorescence originates from the excited states of the two different conformers. The PET from the donor moiety to the acceptor leads to an emissive longer wavelength CT state. In the presence of transition-metal ions, the fluorophore–donor communication is turned off due to the binding of the metal ions at the donor site, thereby leading to the fluorescence enhancement in the LE state and suppression of the longer wavelength CT state.

Experimental Section

All the solvents used were of HPLC grade obtained from Qualigens (India) Ltd. The methylmethacrylate (MMA) was purchased from E. Merck, azobisisobutyronitrile (AIBN) was purchased from Fluka. All the metal perchlorate salts used in the photophysical studies were purchased from Aldrich and Fluka. The methylmethacrylate was extracted with 2 M NaOH solution, washed several times with water, dried over $CaCl_2$, distilled twice under reduced pressure, and then kept at low temperature to prevent polymerisation.
The tetraketone, obtained by the condensation of dimedone and 4-(dimethylamino)benzaldehyde, was treated with ammonium hydroxide in ethanol by the procedure reported in the literature[23] to yield the decahydroacridinedione dye DMAADD.

Absorption spectra were recorded on a Shimadzu UV-1601 UV-VIS spectrophotometer. Fluorescence spectra were recorded using a Perkin-Elmer LS5B luminescence spectrometer. Fluorescence quantum yield were obtained from the corrected fluorescence spectra using Equation (8),

$$\phi_f = (A_s/A_r)(a_s/a_r)(n_s/n_r)^2 \times 0.546 \quad (8)$$

where, A_s and A_r are the area under the corrected fluorescence spectrum, a_s and a_r are the absorbances at the wavelength of excitation (366 nm), and n_s and n_r are the refractive indices of the solvent for the sample and reference, respectively. The absorbance value was adjusted to 0.02. The area under the spectra was obtained by numerically integrating the spectra by Simpson's method. Quinine sulfate in 0.1 N sulfuric acid was used as the reference for quantum yield determination. (ϕ_f of quinine sulphate = 0.546). The 3D emission spectral studies were performed using Hitachi F4500 spectrofluorimeter. The excitation and emission slits were set to 10 nm for all the 3D emission measurements.

Fluorescence decays were recorded using TCSPC method using the following setup. A diode pumped millena CW laser (Spectra Physics) 532 nm was used to pump the Ti:sapphire rod in Tsunami picosecond mode locked laser system (Spectra Physics). The 750 nm (80 MHz) line was taken from the Ti:sapphire laser and passed through a pulse picker (Spectra Physics, 3980 2S) to generate 4 MHz pulses. The second harmonic output (375 nm) was generated by a flexible harmonic generator (Spectra Physics, GWU 23PS). The vertically polarised 375 nm laser was used to excite sample. The fluorescence emission at the magic angle (54.7°) was dispersed in a monochromator (f/3 aperture), counted by a MCP PMT(Hamamatsu R 3809), and processed through CFD, TAC, and MCA. The instrument response function for this system is $\approx$52 ps, and the fluorescence decay was analysed by using the software provided by IBH(DAS-6) and PTI global analysis software. Cyclic voltammograms were obtained on a CH Instruments electrochemical analyser. The measurements were carried out at 100 mV sec^{-1} under oxygen-free conditions using a three-electrode cell in which a glassy carbon electrode was the working electrode, a saturated Ag/AgCl electrode was the reference electrode, and a platinum wire was used as the auxiliary electrode. Tetra(*n*-butyl)ammonium perchlorate was used as the supporting electrolyte.

Acknowledgements

The authors acknowledge Department of Science and Technology and Council of Scientific and Industrial research, India for financial support. We also thank Dr. A. K. Mishra, IIT, Chennai for allowing access to the contour measurement facilities. EJPM is grateful to Professor T. Bally, University of Fribourg, Switzerland for a valuable communication about the MOPLOT software.

Keywords: ab initio calculations · donor–acceptor systems · electron transfer · fluorescence · sensors

[1] E. Lippert, W. Luder, H. Boos in *Advances in Molecular Spectroscopy* (Ed.: A. Mangini), Pergamon Press, Oxford, UK, **1962**, p. 443.
[2] M. C. C. de Lange, D. Thorn Leeson, K. A. B. Van Kuijk, A. H. Huizer, C. A. G. O. Varma, *Chem. Phys.* **1993**, *177*, 243 – 256.
[3] K. Rotkiewicz, K. H. Grellmann, Z. R. Grabowski, *Chem. Phys. Lett.* **1973**, *19*, 315 – 318.
[4] A. L. Sobolewski, W. Domcke, *Chem. Phys. Lett.* **1996**, *250*, 428 – 436.
[5] K. A. Zachariasse, *Chem. Phys. Lett.* **2000**, *320*, 8 – 13.
[6] a) Z. R. Grawbowski, K. Rotkiewicz, W. Rettig, *Chem. Rev.* **2003**, *103*, 3899 – 4031; b) W. Rettig, *Angew. Chem.* **1986**, *98*, 969 – 986; *Angew. Chem. Int. Ed. Engl.* **1986**, *25*, 971 – 988; c) Z. R. Grawbowski, J. Dobkowski, *Pure. Appl. Chem.* **1983**, *55*, 245 – 251; d) A. Siemiarczuk, Z. R. Grawbowski, A. Krowczynski, M. Asher, M. Ottolenghi, *Chem. Phys. Lett.* **1977**, *51*, 315 – 320.
[7] W. Rettig in *Topics in Current Chemistry, Vol. 169* (Ed.: J. Mattay), Springer, Berlin, **1994**, pp. 253 – 299.
[8] a) Y. V. Il'ichev, W. Kuhnle, K. A. Zachariasse, *J. Phys. Chem.* **1998**, *102*, 5670 – 5680; b) K. A. Zachariasse, M. Grobys, T. Von der Haar, Hebecker, Y. V. Il'ichev, Y. B. Jiang, O. Morawski, W. Kuhnle, *J. Photochem. Photobiol. A: Chem.* **1996**, *102*, 59 – 70; c) K. A. Zachariasse, M. Grobys, T. Von der Haar, A. Hebecker, Y. V. Il'ichev, O. Morawski, I. Ruckert, W. Kuhnle, *J. Photochem. Photobiol. A: Chem.* **1997**, *105*, 373 – 383.
[9] V. Balzani, *Electron transfer in Chemistry*, Wiley-VCH, Weinheim, Germany, **2001.**
[10] a) A. P. de Silva, H. Q. N. Gunaratne, T. Gunnlaugsson, A. J. M. Huxley, P. McCoy, J. T. Rademacher, T. E. Rice, *Chem. Rev.* **1997**, *97*, 1515 – 1566; b) *Chemosensors for Ion and Molecule Recognition* (Eds.: A. W. Czarnik, J.-P. Desvergne), Kluwer, Dordrecht, The Netherlands, **1997**.
[11] a) K. J. Prabahar, V. T. Ramakrishnan, D. Sastikumar, S. Sellandurai, V. Masilamani, *Indian J. Pure and Appl. Phys.* **1991**, *29*, 382 – 384; b) P. Shanmugasundaram, K. Joseph Prabahar, V. T. Ramakrishnan, *J. Heterocyclic. Chem.* **1993**, *30*, 1003 – 1007; c) P. Shanmugasundaram, P. Murugan, V. T. Ramakrishnan, N. Srividya, P. Ramamurthy, *Heteroatom Chem.* **1996**, *7*, 17 – 22; d) P. Murugan, P. Shanmugasundaram, V. T. Ramakrishnan, B. Venkatachalapathy, N. Srividya, P. Ramamurthy, K. Gunasekaran, D. Velmurugan, *J. Chem. Soc. Perkin Trans. 2* **1998**, 999 – 1003.
[12] S. Singh, S. Chhina, V. K. Sharma, S. S. Sachdev, *J. Chem. Soc. Chem. Commun.* **1982**, 453 – 454.
[13] a) H. Mohan, N. Srividya, P. Ramamurthy, J. P. Mittal, *J. Phys. Chem. A.* **1997**, *101*, 2931 – 2935; b) H. Mohan, J. P. Mital, N. Srividya, P. Ramamurthy, *J. Phys. Chem. A.* **1998**, 102, 4444 – 4449; c) N. Srividya, P. Ramamurthy, V. T. Ramakrishnan, *Spectrochim. Acta A.* **1998**, *54*, 245 – 253; d) N. Srividya, P. Ramamurthy, V. T. Ramakrishnan, *Spectrochim. Acta A.* **1997**, *53*, 1743 – 1753; e) N. Srividya, P. Ramamurthy, V. T. Ramakrishnan, *Phys. Chem. Chem. Phys.* 2000, *2*, 5120 – 5126; f) V. Thiagarajan, C. Selvaraju, P. Ramamurthy, *J. Photochem. Photobiol. A; Chem.* **2003**, *157*, 23 – 27.
[14] V.Thiagarajan, P.Ramamurthy, unpublished results.
[15] W. Rettig, V. Bonacic-Koutecky, *Chem. Phys. Lett.* **1979**, *62*, 115 – 120.
[16] L. Onsager, *J. Am. Chem. Soc* **1936**, *58*, 1486- 1493.
[17] N. Mataga, T. Kubota, *Molecular Interactions and Electronic Spectra*, Marcel Dekker, New York, **1970**, p. 385.
[18] R. A. Bissell, A. P. de Silva, H. Q. N. Gunaratne, P. L. M. Lynch, G. E. M. Maguire, C. P. McCoy, K. R. A. S. Sandanayake, *Topics in Current Chemistry, Vol. 168*, Springer, Berlin, **1993**, pp. 223 – 264.
[19] Gaussian 03, (Revision B.04), M. J. Frisch, G. W. Trucks, H. B. Schlegel, G. E. Scuseria, M. A. Robb, J. R. Cheeseman, V. G. Zakrzewski, J. A. Montgomery, R. E. Stratmann, J. C. Burant, S. Dapprich, J. M. Millam, A. D. Daniels, K. N. Kudin, M. C. Strain, O. Farkas, J. Tomasi, V. Barone, M. Cossi, R. Cammi, B. Mennucci, C. Pomelli, C. Adamo, S. Clifford, J. Ochterski, G. A. Petersson, P. Y. Ayala, Q. Cui, K. Morokuma, D. K. Malick, A. D. Rabuck, K. Raghavachari, J. B. Foresman, J. Cioslowski, J. V. Ortiz, B. B. Stefanov, G. Liu, A. Liashenko, P. Piskorz, I. Komaromi, R. Gomperts,

R. L. Martin, D. J. Fox, T. Keith, M. A. Al-Laham, C. Y. Peng, A. Nanayakkara, C. Gonzalez, M. Challacombe, P. M. W. Gill, B. G. Johnson, W. Chen, M. W. Wong, J. L. Andres, M. Head-Gordon, E. S. Replogle, J. A. Pople, Gaussian, Inc., Pittsburgh, PA, **2003**.

[20] a) A. D. Becke, *J. Chem. Phys.* **1993**, *98*, 5648 – 5652; b) C. Lee, W. Yang, R. G. Parr, *Phy. Rev. B* **1988**, *37*, 785 – 789.

[21] J. B. Foresman, A. Frisch, *Exploring Chemistry with Electronic Structure Methods*, 2nd edition, Gaussian. Inc., Pittsburgh, PA, **1996**.

[22] a) J. J. P. Stewart, *J. Comp. Chem.* **1989**, *10*, 209 – 220; b) MOPAC 2000, *Molecular orbital Program*, Fujitsu Limited, Tokyo, Japan, **1999**.

[23] V. K. Ganesh, D. Velmurugan, M. Bindya Sagar, P. Murugan, *Acta. Cryst. C* **1998**, *54*, 557 – 559.

[24] a) R. E. Stratmann, G. E. Scuseria, M. J. Frisch, *J. Chem. Phys.* **1998**, *109*, 8218 – 8224; b) R. Bauernschmitt, R. Ahlrichs, *Chem. Phys. Lett.* **1996**, *256*, 454 – 464; c) M. E. Casida, C. Jamorski, K. C. Casida, D. R. Salahub, *J. Chem. Phys.* **1998**, *108*, 4439 – 4449.

[25] C. J. Fahrni, L. Yang, D. G. VanDerveer, *J. Am. Chem. Soc.* **2003**, *125*, 3799 – 3812.

Received: February 14, 2004
Revised: April 8, 2004

